Effects of tetrodotoxin on heart cell aggregates

Phase resetting and annihilation of activity

Alvin Shrier,* John R. Clay,‡ and Richard M. Brochu*

*Department of Physiology, McGill University, McIntyre Medical Building, Montreal, Quebec, Canada H3G 1Y6 and
‡Laboratory of Biophysics, National Institute of Neurological Disorders and Stroke, National Institutes of Health, Bethesda, Maryland 20892 USA

ABSTRACT The influence of relatively low concentrations of tetrodotoxin (TTX) on phase resetting of spontaneous activity of embryonic chick atrial heart cell aggregates by brief duration current pulses was investigated experimentally and theoretically. The maximal upstroke velocity, $\dot{V}_{max}$, of the spontaneous action potential was reduced by TTX in a concentration-dependent manner for [TTX] $< 10^{-7}$ M. However, the beat rate was unaffected in this concentration range. Application of a depolarizing current pulse of brief duration during a critical region of the spontaneous cycle annihilated activity in some preparations exposed to [TTX] $\sim 10^{-7}$ M. These results were analyzed with the model of electrical activity described in the previous paper (Clay, J. R., R. M. Brochu, and A. Shrier. 1990. *Biophys. J.* 58:609–621) based on a tonic block of the I_{Na} channel by TTX with a dissociation constant, K_D, of 50 nM.

INTRODUCTION

Tetrodotoxin (TTX) blocks the inward sodium ion current, I_{Na}, and reduces the associated maximum rate of rise ($\dot{V}_{max}$) of the action potential (AP) of most excitable tissues, such as the heart, including the embryonic chick heart (Narahashi, 1974; Baer et al., 1976; Cohen et al., 1984; Bustamente and McDonald, 1983; McDonald et al., 1972; Ebihara et al., 1980; Fujii et al., 1988; Sada et al., 1988). In particular, it blocks spontaneous activity in embryonic chick heart cell aggregates in a dose-dependent manner in the 10^{-9}–10^{-6} M range and it reduces the maximum rate of rise, $\dot{V}_{max}$, of the action potential (McDonald et al., 1972; Nathan and DeHaan, 1979; Ebihara et al., 1980). That is, the addition of TTX to the external medium is one way to stop spontaneous activity in heart cells. An alternative way is with brief duration current pulses applied shortly after the occurrence of the maximum diastolic potential in the control cycle (Jalife and Antzelevitch, 1979). However, we were unable to stop activity under these conditions in our preparations, as noted in the previous paper, because the equilibrium potential (~ -50 mV) is unstable (Clay et al., 1990). The effects of TTX suggest that a depolarizing current pulse may stop the activity of spontaneously beating aggregates exposed to relatively low doses of this drug. That is, TTX may alter the stability of the equilibrium potential of the current-voltage relation so that the preparation will possess a stable equilibrium point as well as a stable limit cycle. We have specifically tested this hypothesis and we have examined the effects of TTX on phase resetting. We have compared these results with the predictions of our model of spontaneous activity in embryonic chick atrial heart cell aggregates with appropriate modifications in the model to account for the effects of TTX.

Dr. Brochu's current address is Pharmacology Department, Merck-Frosst Inc., PO Box 1005, Pointe-Claire, Dorval, Quebec, Canada, H9R 4P8.

Dr. Clay's mailing address is Laboratory of Biophysics, National Institutes of Health, Building 9, Room 1E124, Bethesda, MD 20892.

METHODS

The experimental preparation of embryonic chick atrial heart cell aggregates and the theoretical techniques used in this study are described in the previous paper (Clay et al., 1990). The $\dot{V}_{max}$ parameter of the action potential was allowed to reach steady state after the addition of tetrodotoxin (Sigma Chemical Co., St. Louis, MO) to the external medium before current pulse studies were initiated, which usually occurred within 15 min.

RESULTS

Basic electrophysiological effects of TTX

The effect of 5×10^{-8} M TTX on spontaneous activity is illustrated in Fig. 1. The maximum upstroke velocity ($\dot{V}_{max}$) of the AP was reduced, as was the AP duration, but the beat rate was strikingly unaffected. The predictions of the model are shown in the right hand panels of Fig. 1 with a reduction of g_{Na} in the model by two-thirds to account for the effect of TTX. Pooled results describing the dual effect of TTX on $\dot{V}_{max}$ and the interbeat interval for several different preparations are shown in Fig. 2. The main conclusion from these results is that $\dot{V}_{max}$ is reduced

0006-3495/90/09/623/07 $2.00

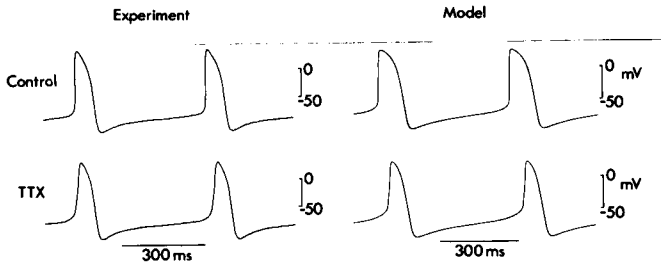

FIGURE 1 Effects of TTX on electrical activity. (*Left*) Control recording of spontaneous activity and effects on this activity of 5×10^{-8} M TTX. (*Right*) Control activity of the model described in Clay et al. (1990) with $I_{b_1} = 0.030$ (V-40), rather than 0.034 (V-40) to closely match the beat rate of the preparation described in the left panel. The I_{Na} component in the model was reduced by two-thirds for the result in the bottom right panel.

in a concentration-dependent manner over the 10^{-9}–10^{-7} M range, but the beat rate is not affected. That is, the preparations either beat, with a rate which is unaltered by TTX, or they are quiescent, especially at higher TTX concentrations. In particular, no spontaneous activity was observed with TTX concentrations higher than 5×10^{-7} M. The theoretical lines in Fig. 2 were obtained from our model of spontaneous activity with the sodium current

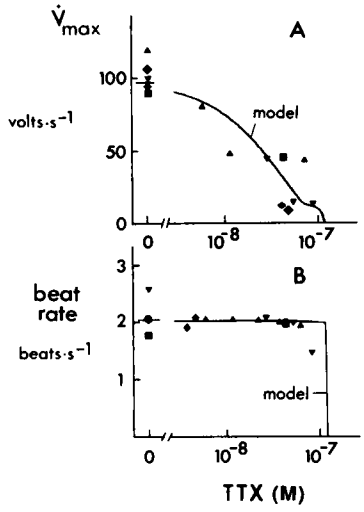

FIGURE 2 Concentration dependence of $\dot{V}_{max}$ and beat rate on [TTX]. (*A*) $\dot{V}_{max}$ (V/s) vs. [TTX] for five different preparations. The theoretical curve was calculated from the model described in the previous paper with the sodium current given by $I_{Na}/(1 + [TTX]/K_D)$, where I_{Na} is the sodium current in control and $K_D = 50$ nM. The experimental results were scaled as follows: 1.0 (♦); 0.71 (▼); 1.95 (▲); 1.5 (♦); and 2.0 (■). (*B*) Beat rate (in beats/s) vs. [TTX] for five experiments, three of which are the same as in *A*. The theoretical curve was calculated from our model. The experimental results were scaled as follows: 1.0 (▼); 0.78 (▲); 0.88 (♦); 1.05 (●); and 1.43 (■).

given by $I_{Na}/(1 + [TTX]/K_D)$, where I_{Na} is given in Table 1 of the previous paper (Clay et al., 1990), [TTX] is the tetrodotoxin concentration, and $K_D = 50$ nM, which provided a good, overall description of our results. The data points in Fig. 2 (and in Fig. 2 alone) have been scaled by a constant factor for each preparation to facilitate the comparison between theory and experiment. The theoretical line in Fig. 2 *A* illustrates a biphasic reduction of $\dot{V}_{max}$ as [TTX] is increased, which is described below (Discussion). The theoretical line in Fig. 2 *B* is consistent with the relative lack of [TTX] on the beat rate. The model predicts a very steep fall off of beat rate with TTX concentration for [TTX] > 10^{-7} M, as described below (Discussion). The effects of TTX on AP parameters are shown in greater detail in Fig. 3. The experimental results in Fig. 3 *A* contain the control AP (trace *a*) from Fig. 1 on an expanded time scale superimposed upon the AP in 5×10^{-8} M TTX (trace *b*). The arrow highlights a slight "hump", or biphasic character of the upstroke in TTX. The $\dot{V}_{max}$ parameter in this preparation was reduced by TTX from 110 to 8 v/s. The AP duration (measured from the overshoot potential to the maximum diastolic potential) was reduced by 15%. The theoretical results shown in Fig. 3 *B* provide a good description of the experimental results, especially the biphasic rising phase of the AP with TTX, although the model predicts a 27% reduction in AP duration, greater than that observed experimentally. A direct comparison of the AP's in TTX is given in Fig. 3 *C*, which contains traces *b* from Fig. 3, *A* and *B*, superimposed upon one another.

Phase resetting

Surprisingly, TTX produced very little effect on phase resetting by brief duration current pulses even when the

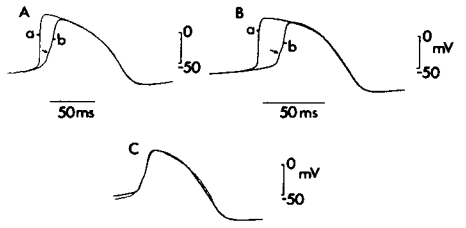

FIGURE 3 (*A*). Comparison of experimental action potential in control (*trace a*) and action potential in 5×10^{-8} M TTX. These results are superimposed so that the repolarization phases overlap as closely as possible. The arrow highlights a biphasic character to the upstroke. (*B*) Comparison of the model action potential in control and with I_{Na} reduced by two-thirds. These results are superimposed so that the repolarization phases overlap as closely as possible. (*C*) Traces *b* in *A* and *B* superimposed upon each other.

$\dot{V}_{max}$ parameter was substantially reduced. For example, we did not observe a clear effect of the drug on the phase-resetting curve (PRC) in three preparations with [TTX] = 0.2–3.0 × 10^{-8} M, even though $\dot{V}_{max}$ was reduced by 40–60% in these experiments. In one other experiment with [TTX] = 2.2 × 10^{-8} M we observed very little effect on the PRC with relatively small current pulses, although we did see an increase by ~50% in the maximal delay of phase resetting, $T_{2,max}/T_0$, with larger amplitude pulses. In another preparation we observed only a 10% increase in this parameter with [TTX] = 4.4 × 10^{-8} M for all pulse amplitudes, even though $\dot{V}_{max}$ was reduced by 80% relative to control. However, the maximal delay was increased by ~300% with relatively large current pulses in this preparation when [TTX] was raised to 6 × 10^{-8} M. An intermediate effect of TTX on phase resetting is illustrated in Fig. 4, which contains the PRC in control and in TTX (7 × 10^{-8} M) for a small pulse amplitude (8 nA; Fig. 4, *A* and *B*) and a moderate pulse amplitude (32 nA; Fig. 4, *C* and *D*). The most prominent effects of the drug, which occurred with 32-nA pulses, were to increase the maximal delay of phase resetting and to shift the time of occurrence of this delay to a slightly earlier time in the unperturbed cycle. The corresponding model results are shown in Fig. 4, *E–H*. An example of the electrical activity in the presence of TTX in this preparation is shown in Fig. 5 for a 32-nA pulse applied on either side of the critical point of the PRC. Note that the overshoot potential of the AP after the current pulse which produced a phase delay was reduced in amplitude by a few millivolts and the overshoot increased a few millivolts for the AP after a pulse which produced a phase advance. The corresponding theoretical results are shown in Fig. 5, *C* and *D*.

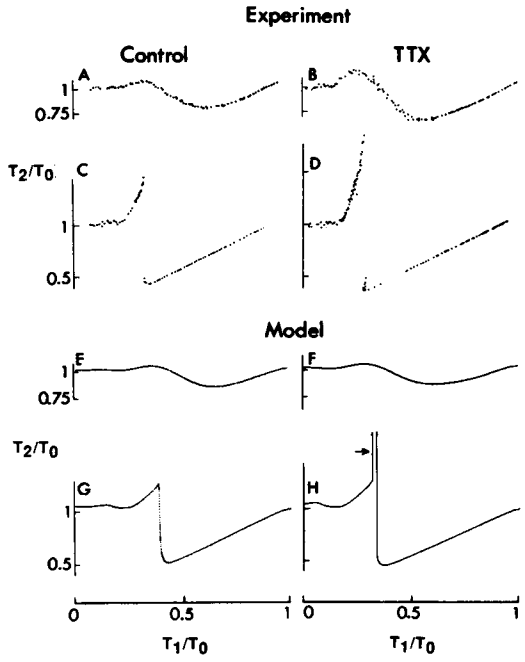

FIGURE 4 Phase-resetting curves in control and in 10^{-7} M TTX. The pulse amplitude was 8 nA in *A, B, E,* and *F;* 32 nA in *C, D, G,* and *H*. The arrow in *H* indicates a ~7-ms region in the unperturbed cycle where the pulse annihilated activity. All results are scaled by the unperturbed cycle length, T_0, as indicated by the labels on the axes, where T_1/T_0 is the relative time in the unperturbed cycle at which the pulse was applied, and T_2/T_0 is the relative time between the AP before and after the pulse.

Annihilation of spontaneous activity by a current pulse

An example of annihilation of spontaneous activity in a TTX-treated preparation ([TTX] = 10^{-7} M) by a current pulse is illustrated in Fig. 6 *A*. A 32-nA depolarizing current pulse 20 ms in duration applied during the initial part of the pacemaker phase of spontaneous activity produced a slight oscillation of the membrane potential subsequent to the pulse, and then, a slow drift (not shown) to a final resting potential of −46 mV. A single depolarizing current pulse could, once again, induce spontaneous activity, as illustrated in Fig. 6 *B*. The overshoot potential and the MDP both grew in amplitude, slightly, during the first few AP's after the pulse. Similar results were obtained in three other preparations. In one of these aggregates the full amplitude of the AP after reinitiation of activity by a current pulse occurred with the first beat after the pulse. We were unable to stop spontaneous activity in another three preparations in which we systematically looked for the effect. That is, we successfully

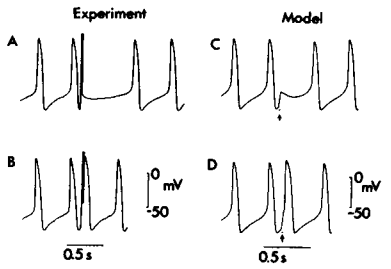

FIGURE 5 Phase resetting with TTX for the preparation described in Fig. 4. (*A*) Maximum delay produced by a 32-nA pulse 20 ms in duration. Note the slight reduction in the overshoot of the first AP after the pulse. (*B*) Phase advance produced by a similar pulse applied 1 ms later in the unperturbed cycle than in *A*. (*C*) Maximum delay (of spontaneous activity) in the model produced by the same pulse conditions as in *A* and *B*. (*D*) Phase advance in the model produced by a similar pulse applied 1 ms later in the unperturbed cycle than in *C*. Note the changes in overshoot in the first AP after the pulse in *C* and *D*. The horizontal bars in *C* and *D*, indicated by the arrows, represent the time during which the pulse was applied in the model.

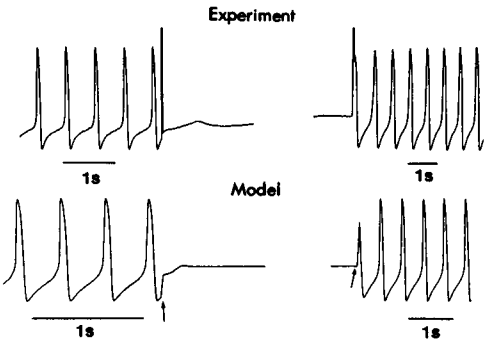

FIGURE 6 (*A*). Annihilation of activity by a 32-nA, 20 ms duration current pulse in the presence of 10^{-7} M TTX. (*B*) Reinitiation of activity from the same preparation as in *A* by 26 nA current pulse 20 ms in duration. The time of the pulse in both *A* and *B* is indicated by the stimulus artifact. (*C*) Theoretical description of cessation of activity in the model with I_{Na} reduced by two-thirds. (*D*) Reinitiation of activity in the model with a 21-nA, 20-ms current pulse. The time of the pulse both in *C* and *D* is indicated by the arrow.

stopped spontaneous activity with a current pulse in four out of seven preparations in TTX ($3 \times 10^{-8} <$ [TTX] $< 1.1 \times 10^{-7}$ M).

The model produced results which were qualitatively similar to our experimental observations (Fig. 6, *C–D*). In particular, a 32-nA current pulse, 20 ms in duration applied during the initial part of the pacemaker phase (indicated by the arrow) caused the membrane potential to oscillate and then finally rest at −54 mV (Fig. 6 *C*). This result is also illustrated in Fig. 4 *H*. The arrow in Fig. 4 *H* indicates a ~7 ms region in the unperturbed cycle for which 32-nA pulses 20 ms in duration abolished activity. That is, the time to the beat subsequent to the pulse is infinite. A single depolarizing current pulse could reinitiate spontaneous activity in the model, as shown in Fig. 6 *D*. The result shown here is for a near threshold current pulse. The first overshoot and MDP of activity were both less than maximal. The full scale AP was achieved by the second cycle of activity after the current pulse.

The main point of this analysis is that the model and some of our preparations both have a stable equilibrium point and a stable limit cycle for relatively low doses of TTX. The comparison between theory and experiment in Fig. 6 does, however, reveal deficiencies in the model. For example, the post-activity oscillation occurred much sooner after the annihilating current pulse in the model than was observed experimentally. Moreover, the model failed to describe the relatively slow recovery of the full amplitude of the action potential after reinitiation of activity by a current pulse.

DISCUSSION

Basic electrophysiology

The effects of TTX on cardiac action potential parameters, the $\dot{V}_{max}$ parameter in particular, have received considerable attention (Baer et al., 1976; Cohen et al., 1984; Watanabe and McDonald, 1986). We observed a biphasic upstroke of the AP with [TTX] $\sim 5 \times 10^{-8} - 10^{-7}$ M, an effect which does not appear to have been reported previously. Our theoretical analysis demonstrates that this result is attributable to the relative contributions of I_{Na} and I_{Ca} to the upstroke. Moreover, I_{Ca}, together with I_{Na}, is responsible for the biphasic nature of the $\dot{V}_{max}$ vs. [TTX] theoretical relationship in Fig. 2 *A* for [TTX] $> 8 \times 10^{-8}$ M. That is, $\dot{V}_{max}$ is reduced with increasing TTX concentration until the rate of depolarization generated by I_{Ca} exceeds the rate of depolarization generated by I_{Na}. The role of I_{Na} under these conditions is to depolarize the membrane to the threshold of I_{Ca} (~ −30 mV), which then generates the remaining portion of the upstroke phase of the AP. The further reduction of $\dot{V}_{max}$ for [TTX] $> 10^{-7}$ M is attributable to the very slow rate at which I_{Na} depolarizes the membrane toward the I_{Ca} threshold. The inactivation of the I_{Ca} component becomes significant under these conditions, which reduces the amount of I_{Ca} available for activation. No spontaneous activity occurs in the model for [TTX] $> 1.2 \times 10^{-7}$ M because no mechanism exists to depolarize the membrane to the threshold of I_{Ca} under these conditions.

The ionic mechanism underlying the reduction of action potential duration (APD) in the model with TTX (Fig. 3) is illustrated in Fig. 7. The contributions of I_{Na} in control (trace *a*) and with 10^{-7} M TTX (trace *b*) are shown below the action potentials for these conditions, which are superimposed in the top panel of Fig. 7. The I_{Ca} results in Fig. 7 reveal a surprising prediction of the model. The peak I_{Ca} amplitude and the net Ca^{+2} influx during the upstroke in 10^{-7} M TTX are both greater in TTX than in control. The reason for this result is that the upstroke velocity is reduced, thereby allowing the I_{Ca} component more time to activate. This increase in I_{Ca} causes a greater transient increase in the internal Ca^{+2} than in control, thereby increasing the calcium current inactivation parameter in the model, f' (Fischmeister and Horackova, 1983; Kass and Sanguinetti, 1984; Lee et al., 1985; Shrier and Clay, 1986). That is, the reduction in the overshoot potential and action potential duration in the model with TTX are both caused, paradoxically, by an increase in I_{Ca}. The decrease in APD is offset by the increase in time which the membrane takes to reach the I_{Ca} threshold so that the overall interbeat interval is

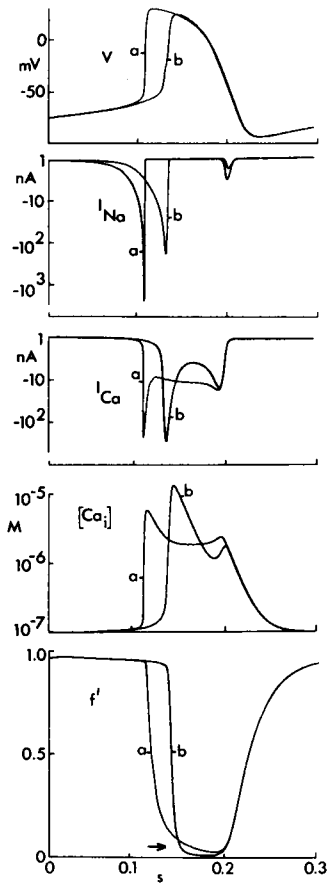

FIGURE 7 Reduction in overshoot potential and action potential duration with a two-thirds reduction in I_{Na} to simulate the effect of 10^{-7} M TTX on the action potential in the Shrier and Clay (1986) model. The control and TTX records, labeled *a* and *b*, respectively, are shown superimposed so that the repolarization phases overlap as much as possible. The sodium and calcium ion currents during each simulation are shown in the two panels below the action potentials, and the internal calcium ion concentration and the calcium ion current dependent inactivation parameter, f', are shown in the two bottom panels. (The quantities which are plotted in the I_{Na} and I_{Ca} panels are actually $-\log [\text{abs}(I_{Na}) + 1]$ and $-\log [\text{abs}(I_{Ca}) + 1]$, respectively). The I_{Ca} component is actually greater during the upstroke in TTX, as described in the text, which leads to a greater transient increase in $[Ca^{+2}]_i$ and consequently greater inactivation, as illustrated by the arrow in the bottom panel. This mechanism accounts for the reduction in the overshoot and APD in the model.

relatively unchanged by TTX, even when I_{Na} is significantly suppressed (Fig. 2 *B*). The very steep fall off of beat rate with [TTX] in the model occurs when I_{Na} is reduced to the point that it can no longer depolarize the membrane to the threshold of I_{Ca}, as noted above. The overall emphasis on I_{Ca} in this analysis relative to the previous paper is due simply to the fact that when I_{Na} is depressed, I_{Ca} becomes a much greater factor during the upstroke than in control. The outward currents in the model AP are relatively unaffected, because the overshoot of the AP is nearly the same in 10^{-7} M TTX as in control.

We found that K_D = 50 nM provided a good description of our TTX results, where K_D is the dissociation constant for the effect of the drug on the I_{Na} channel (half-maximal block of I_{Na}). This value is to be contrasted with K_D = 1 nM reported by Fujii et al. (1988) for 3–7 d old embryonic chick heart cells based upon voltage clamp measurements of I_{Na}, and with K_D = 10 nM for the reduction of $\dot{V}_{max}$ with TTX from either the embryonic or the adult chick heart reported by Marcus and Fozzard (1981). All three results are considerably smaller than the 8–22 μM range for this parameter which has been reported for adult mammalian cardiac myocytes (Watanabe and McDonald, 1986). Moreover, the block of I_{Na} by TTX in embryonic chick myocytes is voltage independent (Fujii et al., 1988; Sada et al., 1988) and the reduction of $\dot{V}_{max}$ by TTX is frequency independent (A. Shrier, unpublished). Both of these results also differ from the effect of the drug on the mammalian cardiac I_{Na} channel. In fact, the I_{Na} channel in embryonic chick cardiac myocytes appears to be similar to the neuronal I_{Na} channel with regard to TTX action. The neuronal I_{Na} channel also lacks a frequency dependence of TTX block with a K_D in the nanomolar range (Narahashi, 1974).

Phase resetting and annihilation of activity

The effects of TTX on phase resetting of spontaneous activity are relatively subtle, which is surprising in view of its substantial effect on I_{Na}. The drug shifted the critical point, slightly, to earlier times in the control cycle and increased the maximal delay of the time of occurrence of the AP subsequent to the pulse (Fig. 4). The former effect is related to the decrease in AP duration caused by the drug. The interplay between I_{Na} and I_{x_1} subsequent to the current pulse, which is described in the previous paper, is similar in this analysis even though I_{Na} is significantly reduced. The threshold of I_{Na} activation is unchanged by TTX. Consequently, the same amplitude and timing of a pulse subsequent to MDP will be required to depolarize the membrane potential to threshold as in control. The main effect of TTX, the increase in the maximal delay, is attributable to the equilibrium point, which is unstable in control conditions. This instability can be removed by TTX, an effect which is dramatically illustrated by the annihilation of activity with a current pulse (Fig. 4 *H;* Fig. 6 *A*). The slight oscillation subsequent to the pulse illustrated in Fig. 6 *A* is, according to the model analysis (Fig. 6 *B*), attributable to incomplete activation of the I_{Na} component which remains in the presence of submaximal

doses of TTX. This current begins to depolarize the membrane potential toward threshold of I_{Ca} after the pulse, but it does so in such a slow fashion that it inactivates, thereby allowing I_{x_1} and I_b to cause a slight hyperpolarization after failure to reach the I_{Ca} threshold. The slow drift in membrane potential toward the resting potential after this oscillation (Fig. 6 *A*) is unexplained by the model, as is the increase in AP amplitude during the first four AP's after the triggering pulse (Fig. 6 *B*).

Phase plane analysis

The current-voltage trajectory of the limit cycle oscillation of the model with a two-thirds reduction of I_{Na} is shown in Fig. 8. The two inward current features of this trajectory illustrate the contributions of I_{Na} and I_{Ca} underlying the biphasic nature of the upstroke (Fig. 3). The model also possesses a stable equilibrium point, or resting potential at $V = \sim -54$ mV, and an unstable limit cycle. (The equilibrium potential is hyperpolarized by TTX from -51 to -54 mV, because of the reduction in the I_{Na} window current.) That is, the model (and some of our preparations) have two stable features; a stable point and a stable limit cycle. Each feature has a region of attraction in phase space. That is, the membrane potential will return to the limit cycle after a perturbation away from this feature, unless the perturbation is of sufficient strength and duration to switch the system to its equilibrium point. For example, the model can be switched from the limit cycle to the resting potential with 32 nA, 20-ms duration pulses provided that such a pulse is applied during the portion of the cycle illustrated by the small bar between ~ -90 and -88 mV in Fig. 8 (denoted by the arrows in Fig. 8). This region of the cycle corresponds to the $\sim$ 7-ms region of the phase response curve in Fig. 4 *H* for which the time of the beat subsequent to the pulse is infinite. An example of the change of state between the two stable features of the model is illustrated in the inset below the limit cycle in Fig. 8, which shows the portion of the cycle during the latter part of repolarization and the pacemaker phase, as well as the trajectory during the pulse (the dashed line in the inset of Fig. 8) and the trajectory after the pulse. The latter trajectory spirals toward the equilibrium point. The electrical response associated with this result is shown above the limit cycle. Similar pulses applied outside of the -90 to -88 mV range of the unperturbed cycle will not stop activity. Under these conditions the model will return to the limit cycle. Similarly, small amplitude pulses are not sufficient to switch the system from the limit cycle to the equilibrium point, regardless of where they are applied during the unperturbed cycle. Consequently, our failure to stop activity in all preparations, noted above, is not surprising. The conditions required for this effect to occur are narrowly constrained even in the model.

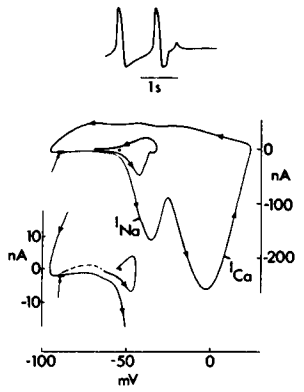

FIGURE 8 Current-voltage limit cycle, or phase plane, analysis of the model with a two-thirds reduction of I_{Na}. The arrows on the trajectories indicate the direction of time. The smaller limit cycle within the unperturbed cycle is an approximation to an unstable limit cycle which the model also possesses. An example of annihilation of activity in the model is illustrated above the limit cycle. This result is also illustrated by the inset below (on the same voltage scale and an expanded current scale). The latter part of repolarization and the pacemaker phase are shown, as well as the trajectory during the current pulse (*dashed line*) and the trajectory after the pulse. The symbol (●) within the limit cycle and in the inset below represents the resting or equilibrium point in the model. The bar alongside of the early pacemaker phase of the cycle (denoted by the arrow) represents the region of the unperturbed cycle for which 32-nA 20-ms duration pulses annihilate activity.

Comparison with other work

Our analysis is similar to that of Guttman et al. (1980) and Chapman (1980). Both reports demonstrated annihilation of firing with a single current pulse in squid axons made to fire repetitively either by exposure to seawater containing reduced levels of calcium ions (Guttman et al., 1980) or by application of steady depolarizing current (Chapman, 1980). Guttman et al. (1980) analyzed their results with the Hodgkin and Huxley (1952) model of squid axon currents with a steady, depolarizing bias current to produce repetitive activity. The Hodgkin and Huxley (1952) model possesses a stable equilibrium point and a stable limit cycle under these conditions (Guttman et al., 1980).

Annihilation of spontaneous activity by a single depolarizing current pulse has been reported in the sino-atrial node and in Purkinje fibers (Jalife and Antzelevitch, 1979, 1980), and in the diseased human heart under certain clinical conditions (Gilmour et al., 1983). We have illustrated the influence of a specific ion channel blocker, TTX, on this phenomenon. Our results are consistent with the observation by Best (1979) and Van Meerwijk et al. (1984) that cardiac pacemakers and,

indeed, cellular pacemakers in general fall into two categories: autonomous pacemakers, those which cannot be stopped without a steady, continuous influence, such as hyperpolarizing current; and triggered pacemakers, those which can be stopped with a perturbation of brief or finite duration (Best, 1979; Van Meerwijk et al., 1984). One type of pacemaker can be transformed to the other type with a steady bias current (Best, 1979). Our results demonstrate that this transformation can also be accomplished with an ion channel blocker.

We gratefully acknowledge the assistance of Josee Morisette and Laurie Sehn in some experiments.

This work was supported by grants to Dr. Shrier from the Quebec Heart and Stroke Foundation and the Medical Research Council of Canada.

Received for publication 5 January 1990 and in final form 2 May 1990.

REFERENCES

Baer, M., P. M. Best, and H. Reuter. 1976. Voltage-dependent action of tetrodotoxin in mammalian cardiac muscle. *Nature (Lond.).* 263:344–345.

Best, E. N. 1979. Null space in the Hodgkin-Huxley equations. A critical test. *Biophys. J.* 27:87–104.

Bustamente, J. O., and T. F. McDonald. 1983. Sodium currents in segments of human heart cells. *Science (Wash. DC).* 220:320–321.

Chapman, R. A. 1980. Repetitive responses in squid giant axons and their premature annihilation by additional brief depolarizing currents. *Q. J. Exp. Physiol.* 65:1–7.

Clay, J. R., R. M. Brochu, and A. Shrier. 1990. Phase resetting of embryonic chick atrial heart cell aggregates. Experiment and theory. *Biophys. J.* 58:609–621.

Cohen, C. J., B. P. Bean, and R. W. Tsien. 1984. Maximal upstroke velocity as an index of available sodium conductance. Comparison of maximal upstroke velocity and voltage clamp measurements of sodium current in rabbit Purkinje fibers. *Circ. Res.* 54:636–651.

Ebihara, L., N. Shigeto, M. Lieberman, and E. A. Johnson. 1980. The initial inward current in spherical clusters of chick embryonic heart cells. *J. Gen. Physiol.* 75:437–456.

Fischmeister, R., and M. Horackova. 1983. Variation of intracellular Ca^{+2} following Ca^{+2} current in heart. A theoretical study of ionic diffusion inside a cylindrical cell. *Biophys. J.* 41:341–348.

Fujii, S., R. K. Ayer, and R. L. DeHaan. 1988. Development of the fast sodium current in early embryonic chick heart cells. *J. Membr. Biol.* 101:209–223.

Gilmour, R. F., Jr., J. J. Heger, E. N. Prystowsky, and D. P. Zipes. 1983. Cellular electrophysiologic abnormalities of diseased human ventricular myocardium. *Am. J. Cardiol.* 51:137–144.

Guttman, R., S. Lewis, and J. Rinzel. 1980. Control of repetitive firing in squid axon membrane as a model for a neuroneoscillator. *J. Physiol. (Lond.).* 305:377–395.

Hodgkin, A. L., and A. F. Huxley. 1952. A quantitative description of membrane current and its application to conduction and excitation in nerve. *J. Physiol. (Lond.).* 117:500–544.

Jalife, J., and C. Antzelevitch. 1979. Phase resetting and annihilation of pacemaker activity in cardiac tissue. *Science (Wash. DC).* 206:695–697.

Jalife, J., and C. Antzelevitch. 1980. Pacemaker annihilation: diagnostic and therapeutic implications. *Am. Heart J.* 100:128–130.

Kass, R. S., and M. C. Sanguinetti. 1984. Calcium channel inactivation in the calf cardiac Purkinje fiber: evidence for voltage- and calcium-mediated mechanisms. *J. Gen. Physiol.* 84:705–726.

Lee, K. S., E. Marban, and R. W. Tsien. 1985. Inactivation of calcium channels in mammalian heart cells. *J. Physiol. (Lond.).* 364:395–411.

Marcus, N. C., and H. Fozzard. 1981. TTX sensitivity in the developing and adult chick heart. *J. Mol. Cell. Cardiol.* 13:335–340.

McDonald, T. F., H. G. Sachs, and R. L. DeHaan. 1972. Development of sensitivity to tetrodotoxin in beating chick embryo hearts, single cells, and aggregates. *Science (Wash. DC).* 176:1248–1250.

Narahashi, T. 1974. Chemicals as tools in the study of excitable membranes. *Physiol. Rev.* 54:813–889.

Nathan, R. D., and R. L. DeHaan. 1979. Voltage-clamp analysis of embryonic heart cell aggregates. *J. Gen. Physiol.* 73:175–198.

Sada, H., M. Kojima, and N. Sperelakis. 1988. Fast inward current properties of voltage-clamped ventricular cells of embryonic chick heart. *Am. J. Physiol.* 255:H540–H553.

Shrier, A., and J. R. Clay. 1986. Repolarization currents in embryonic chick atrial heart cell aggregates. *Biophys. J.* 50:861–874.

Van Meerwijk, P. M. W., G. DeBruin, A. C. G. Van Ginneken, J. Vanhartevelt, H. J. Jongsma, E. W. Kruyt, S. S. Scott, and D. L. Ypey. 1984. Phase resetting properties of cardiac pacemaker cells. *J. Gen. Physiol.* 83:613–629.

Watanabe, T., and T. F. McDonald. 1986. Tetrodotoxin exerts a large frequency-dependent depression of the maximum rate of rise of action potential in guinea pig ventricular myocytes. *Pfluegers Archiv. Eur. J. Physiol.* 406:645–647.